

Third Order Nonlinear Optical Properties of Squaraine Dyes Having Absorption below 500 nm: A Combined Experimental and Theoretical Investigation of Closed Shell Oxyallyl Derivatives

Ch. Prabhakar,^{†,‡} K. Bhanuprakash,^{*,†} V. Jayathirtha Rao,^{*,‡} M. Balamuralikrishna,[§] and D. Narayana Rao^{*,§}

Inorganic and Physical Chemistry Division, Organic Chemistry Division, Indian Institute of Chemical Technology, Hyderabad 500 607, and School of Physics, University of Hyderabad, Hyderabad 500 046, India

Received: September 2, 2009; Revised Manuscript Received: March 3, 2010

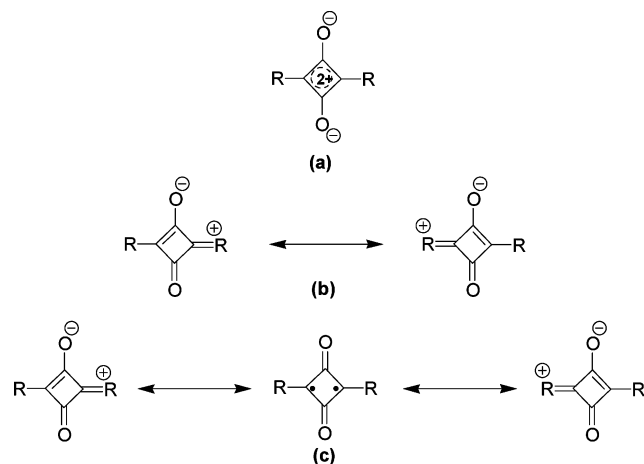
Nonlinear optical (NLO) activity of a molecule in general is connected to fundamental issues like charge transfer, conjugation, polarization, and recently suggested and less investigated diradical character. Extensively studied molecules for negative second order hyperpolarizabilities are the centrosymmetric squaraine derivatives (SQ) which have absorption in the region greater than 600 nm. These have no formal electronic structure but can be represented as a mixture of zwitterionic and diradicaloid valence bond resonance structures. In this work we have designed and synthesized arylamino SQ, **1–10**, which bias the valence bond resonance picture completely to the zwitterionic type and totally eliminates the diradicaloid contribution (estimated using computational studies to be zero). Due to this, the lowest energy transitions are blue-shifted to the region less than 500 nm. We have carried out degenerate four wave mixing (DFWM) studies for estimation of γ values of these molecules using a 800 nm wavelength laser. The γ values are measured under nonresonant conditions and also at intensities where two photon absorption does not play any role. Nonlinear absorption properties of these molecules are studied through Z scan technique. The γ values, though smaller than the SQ having absorption in the red region, are reasonably large and range from -1.2 to -6.9×10^{-33} esu. High level computational techniques and model molecules have been utilized to understand the transition and the NLO activity in these molecules.

Introduction

Nonlinear optics (NLO) deals with the interaction of applied electromagnetic fields (like laser light) in various materials to generate new electromagnetic fields altered in frequency, phase, or other physical properties.^{1–8} This field has attracted lot of interest in the past two decades not only because of the numerous possible applications in telecommunications, dynamic holography, frequency mixing, optical data storage, and so forth, but also because of the fundamental science connected to issues like charge transfer, conjugation, polarization, and recently suggested diradical character.^{9–13} Owing to the combination of chemical tunability, choice of synthetic strategies, and ultrafast response time, organic molecules in particular have received much attention. In fact synthesis, characterization, and modeling of new organic molecules for second and third order NLO is a very active field.^{14–21} For the third order NLO property of organic molecules, studies have been carried out under both resonance and nonresonance conditions with the former yielding values which are 1–2 orders of magnitude larger than the latter.

A widely studied molecular material for the negative third order NLO is the centrosymmetric squaraine (SQ) with various substitutions.¹⁸ SQ dyes are novel class of organic dyes that play a crucial role in the development of various types of materials for the applications such as nonlinear optics, electro-

SCHEME 1: Squaraine Represented (a) as D-A-D, (b) by Valence Bond Zwitterionic Contributions,^a and (c) when Diradical Contribution Is Not Zero



^a Not all possible zwitterionic structures are shown.

photography, xerography, photovoltaics, chemo sensors, biological labeling, and photodynamic therapy.²² There has been a lot of interest in these molecules in the last two decades due to these varied applications and their unique photophysical properties.^{18,22,23} As the molecule has a non-Kekule structure the conventional representation of SQ dyes is a donor–acceptor–donor (D-A-D) type of structural arrangement as shown in Scheme 1a. The valence bond (VB) resonance representation for this is shown in scheme 1b. In general, this type of structural

* Corresponding authors. E-mail: bhanu2505@yahoo.co.in; jrao@iict.res.in; dnrsp@uohyd.ernet.in.

[†] Inorganic and Physical Chemistry Division, Indian Institute of Chemical Technology.

[‡] Organic Chemistry Division, Indian Institute of Chemical Technology.

[§] University of Hyderabad.

arrangement is known as symmetrical SQ dye derivatives, and it is assumed that on excitation charge transition takes place from the side donor groups to the central acceptor part.^{23f} Many studies with a change of the donor group to improve the absorption properties have been reported.^{24,25} High-level theoretical studies of the symmetric squaraines have been reported which give us some idea of the structure, bonding and transitions in these molecules.^{11a,13a} Bigelow and Freund have carried out a comparative study of bis(4-dimethyl aminophenyl) squaraine with bis(dimethylamino)undecamethine using MNDO and CNDO/S (S+DESCI) semiempirical methodologies.²⁶ Comparing the geometry of the squaraine with the cyanine molecule they found that the squaraine has a tendency to have a distinctly polyene like structure or single–double bond length alternation which is in contrast to polymethine behavior. The charge transfer in the excited state is also seen to be larger from the oxygen atoms, (which act as electron acceptors in the ground state) than the donor groups attached to the ring. They conclude that the aromatic or cyanine like model is insufficient to reflect the squaraine's excited state properties. Gude and Rettig carried out combined experimental and computational investigation of some SQ dyes.²⁷ They concluded that the SQ dyes studied by them cannot be directly compared to push–pull cyclobutadienes or cyanines. Ros-Lis et al. in a recent study have suggested that the SQ dyes have more polymethinic than intra molecular charge transfer character.²⁸

Fabian and Zahradnik had proposed an alternate concept to understand the transition occurring in near-infrared (NIR) dyes.^{29a} This is based on the diradicaloid character of the molecule. Molecules which have approximately degenerate non bonding molecular orbitals that are occupied by two electrons are called diradicaloids.^{29b} The diradicaloid character of the molecule can be determined theoretically either from the S^2 values obtained from the spin-broken symmetry (BS) DFT/HF calculations or from the occupation numbers (vide infra).^{29c} For a long chain polymethine type of molecule, the diradicaloid character would be almost zero.^{29a,b} We have used this model to explain the red-shift observed in the absorption in the NIR oxyallyl dyes due to substitutions.^{11a,13} In this model, the squaraine would be viewed as having a VB resonance structures as shown in Scheme 1c. Here in addition to the zwitterionic structures an extra diradical structure also contributes.²⁸ We have reported recently using high level SAC–CI and DFT/TDDFT methodologies that there is direct correlation of the NIR absorption to the diradical character and not to the donor strength of the groups attached to the central ring in these oxyallyl dyes.^{11a,b,12,13} The larger the contribution of the diradicaloid component to the resonance, larger would be the red shift to the NIR region.

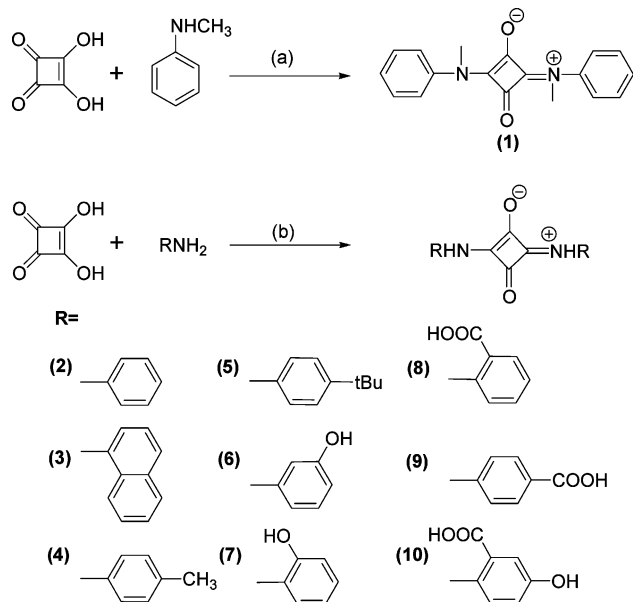
In the past two decades there has been a lot of investigation both experimental and theoretical into the effect of conjugation, donor–acceptor strength, and charge transfer on the NLO activity of organic molecules.^{30–32} In continuation of our interest in the NLO activity of oxyallyl derivatives, we report in this work the synthesis and characterization of new visible absorbing squaraine dyes.¹² We chose molecules with various arylamino donating groups attached to oxyallyl ring. The novelty of these molecules is that these have no diradical character and with the break in conjugation due to direct bonding of the donating group to the ring these bias the resonance to the zwitterionic electronic structure.^{29a} Compared to our earlier report of croconates and other reports of NIR SQ, which can be represented by VB structure Scheme 1c, the molecules being reported here have VB structure as shown in Scheme 1b. Thus

the amino groups would act as a strong donors in addition to the donor oxygen atoms attached to the ring. These dyes have absorption maxima between 387 and 442 nm in dimethylformamide (DMF). We determine the third order nonlinear properties of these squaraines using degenerate four wave mixing (DFWM) method and high level computational techniques. To the best of our knowledge, this is the first report on the NLO activity of a series of squaraine dyes which have absorption below 500 nm.

Experimental Section

Materials and Instruments. Squaric acid was purchased from Aldrich. All other reagents were A.R. grade and used without purification. ^1H NMR spectra were recorded on 300 and 400 MHz spectrophotometers in DMSO, CDCl_3 with TMS as standard, ^{13}C NMR spectra were recorded on 100 MHz spectrophotometer in CDCl_3 with TMS as a standard. IR spectra were taken on a SHIMADZU 435 infrared spectrophotometer. UV–visible absorption spectra were measured on a Jasco V-550 spectrophotometer. Mass spectra were obtained by using electro spray ionization iontrap mass spectrometry (ThermoFinnigan, Sanzox, CA). High resolution mass spectra (HRMS) were carried out by using electro spray ionization quadrupole time-of-flight (ESI Q Tof) mass spectrometry (QSTAR XL, Applied biosystems/MSD sciex, Fostercity, USA). Elemental analyses were performed using a Vario-EL elemental analyzer. Thermogravimetric analysis (TGA) was performed using TGA/SDTA 851° in the temperature range of 25–500 °C in a nitrogen atmosphere at a heating rate of 10 °C min⁻¹.

The third order nonlinear optical studies were carried out by the DFWM method. Ultrashort laser pulses used in the present study were obtained from a conventional chirped pulse amplification (CPA) system comprising of an oscillator (Maitai, Spectra-Physics Inc.) that delivers a ~80 fs, 82 MHz pulse train with pulse energy of 1 nJ at 800 nm and a regenerative amplifier (Spitfire, Spectra Physics Inc.), pumped by a 150 ns, 1 kHz, Q-switched Nd: YLF laser. After regenerative amplification, we obtained amplified pulses of pulse width ~100 fs determined by second order intensity autocorrelation with output energy of up to 1 mJ, at 1 kHz repetition rate. The DFWM setup used was in box-car geometry.^{6b} In brief, in a box-car arrangement the fundamental beam is divided into three nearly equal intensity beams in such a way that the three form three corners of a square box and are focused into the nonlinear medium (sample) both spatially and temporally. The resultant DFWM signal that comes as the fourth corner of the box generated as a result of the phase-matched interaction $k_4 = k_3 - k_2 + k_1$ of the three incident beams. The sample under consideration is taken in the form of solution filled in a 1 mm glass cuvette. Care was taken to reduce the contribution of the cuvette toward the overall DFWM signal by choosing suitable focusing conditions. By maintaining same polarization for the three incident beams we estimated $\chi_{111}^{(3)}$. A half-wave plate was introduced in the path of beam-2 to have its polarization perpendicular to that of beam-1 and beam-3 so that we could estimate $\chi_{1212}^{(3)}$. The transient DFWM profiles for the sample were obtained by delaying the beam-3 with respect to the other two incident beams. By performing the nonlinear transmission experiments on the sample, the input powers for the three input pulses were chosen such that effect of nonlinear absorption can be neglected and hence the obtained DFWM signal contains purely instantaneous nonlinear response of the sample. The obtained $\chi^{(3)}$ data is hence purely real in nature without any contribution of imaginary components due to multiphoton absorption. Also the choice of

SCHEME 2: Reaction Conditions (a) in Methanol Reflux for 4 h (b) in Methanol Reflux for 40–90 min

low input powers allows us to neglect the contribution of higher order nonlinearities. Since all the samples show no absorption at the laser wavelength (800 nm), we expect $\chi^{(3)}$ and γ values are non resonant.

Synthesis and Characterization. General Procedure for the Preparation of 1,3-Disubstituted Squaraines (1–10; Scheme 2). Squaraine dyes were synthesized by taking 2.0 mmol (228 mg) of squaric acid dissolved in 10 mL of hot methanol, to this solution 4.0 mmol of aniline/substituted aniline/*N*-methylaniline/naphthalene (1:2 ratio) was added at 60 °C. Reaction mixture was refluxed for 40–90 min. In case of 1 reaction mixture was refluxed for four hours. The precipitated solid was filtered through Buckner funnel and washed with hot MeOH (10 mL portions 3 times). Yields: 13–65%.³³

1. *Isolated Yield 51%; MP: 183–186 °C.* ¹H NMR(CDCl₃) δ : 3.89 (s, 3H), 3.93 (s, 3H), 7.21–7.43 (m, 10H); ¹³C NMR(CDCl₃) δ : 177.2, 171.2, 168.9, 166.5, 140.9, 140.7, 128.9, 126.9, 122.6, 38.7, 38.3; MS (ESI): m/z 293 (M+H)⁺; IR(KBr): 2361 cm⁻¹ (N–CH₃), 1616 cm⁻¹ (C=O); HRMS (m/z): [M+H] Calculated for C₁₈H₁₆N₂O₂, 293.1297, found, 293.1290. Elemental analysis for C₁₈H₁₆N₂O₂: Found: C, 73.76; H, 5.37; N, 9.42%; requires C, 73.95; H, 5.58; N, 9.58%.

2. *Isolated Yield 56%; MP: > 300 °C.* ¹H NMR(DMSO-*d*₆) δ : 7.41–7.45 (m, 6H), 7.53–7.55 (d, 4H), 11.44 (s, 2H); MS (ESI): m/z 265 (M+H)⁺; IR(KBr): 3179 cm⁻¹ (NH), 1788 (C=O); HRMS (m/z): [M+Na] Calculated for C₁₆H₁₂N₂O₂Na, 287.0791, found, 287.0796. Elemental analysis for C₁₆H₁₂N₂O₂: Found: C, 72.33; H, 4.61; N, 10.49%; requires C, 72.71; H, 4.58; N, 10.6%.

3. *Isolated Yield 38%; MP: >300 °C.* ¹H NMR(DMSO-*d*₆) δ : 7.53–7.61 (m, 8H), 7.82–7.87 (m, 2H), 7.96–8 (m, 2H), 8.15–8.19 (m, 2H), 11.69 (b, 2H); MS (ESI): m/z 365 (M+H)⁺; IR(KBr): 3057 cm⁻¹ (NH), 1617 cm⁻¹ (C=O); HRMS (m/z): [M+Na] Calculated for C₂₄H₁₆N₂O₂Na, 387.1114, found, 387.1109. Elemental analysis for C₂₄H₁₆N₂O₂: Found: C, 78.68; H, 4.45; N, 7.35%; requires C, 79.11; H, 4.43; N, 7.68%.

4. *Isolated Yield 26%; MP: > 300 °C.* MS (ESI –ve mode): m/z 291 (M-1)⁺; IR (KBr): 3178 cm⁻¹ (NH), 1577 cm⁻¹ (C=O). Elemental analysis for C₁₈H₁₆N₂O₂: Found: C, 73.56; H, 5.46; N, 9.27%; requires C, 73.95; H, 5.52; N, 9.58%.

5. *Isolated Yield 13%; MP: > 300 °C.* MS (ESI –ve mode): m/z 375 (M-1)⁺; IR (KBr): 3171 cm⁻¹ (NH), 1579 cm⁻¹ (C=O). Elemental analysis for C₂₄H₂₈N₂O₂: Found: C, 76.18; H, 7.58; N, 7.62%; requires C, 76.56; H, 7.5; N, 7.44%.

6. *Isolated Yield 22%; MP: > 300 °C.* ¹H NMR(DMSO-*d*₆) δ : 6.52–6.54 (d, 2H, *J* = 7.77), 7.12–7.28 (m, 6H), 9.6 (s, 2H), 10.08 (b, 2H), 11.25 (s, 2H); MS (ESI –ve mode): m/z 295 (M-1)⁺; IR(KBr): 3186 cm⁻¹ (NH), 1586 cm⁻¹ (C=O). Elemental analysis for C₁₆H₁₂N₂O₄: Found: C, 64.65; H, 4.18; N, 9.41%; requires C, 64.86; H, 4.08; N, 9.46%.

7. *Isolated Yield 17%; MP: 279–283 °C.* ¹H NMR(DMSO-*d*₆) δ : 6.79–6.88 (m, 4H), 6.99–7.05 (m, 2H), 7.61–7.64 (m, 2H), 10.08 (b, 2H), 10.12 (s, 2H); MS (ESI –ve mode): m/z 295 (M-1)⁺; IR(KBr): 3271 cm⁻¹ (NH), 1635 cm⁻¹ (C=O). Elemental analysis for C₁₆H₁₂N₂O₄: Found: C, 64.44; H, 4.15; N, 9.55%; requires C, 64.86; H, 4.08; N, 9.46%.

8. *Isolated Yield 65%; MP: >300 °C.* ¹H NMR(DMSO-*d*₆) δ : 6.52–6.55 (t, 1H, *J* = 8.057), 6.75–6.77 (d, 1H, *J* = 8.057), 7.03–7.07 (t, 1H, *J* = 8.057), 7.22–7.26 (t, 1H, *J* = 7.162), 7.57–7.61 (t, 1H, *J* = 7.162), 7.68–7.7 (d, 1H, *J* = 7.162), 7.93–7.95 (d, 1H, *J* = 7.162), 8.14–8.16 (d, 1H, *J* = 7.162), 10.92 (s, 2H), 12.11 (b, 2H); MS (ESI –ve mode): m/z 351 (M-1)⁺; IR(KBr): 3162 cm⁻¹ (NH), 1796 cm⁻¹ (C=O). Elemental analysis for C₁₈H₁₂N₂O₆: Found: C, 60.91; H, 3.65; N, 7.86%; requires C, 61.37; H, 3.43; N, 7.95%.

9. *Isolated Yield 63%; MP: > 300 °C.* ¹H NMR(DMSO-*d*₆) δ : 7.82–7.95 (m, 8H), 11.87 (s, 2H); MS (ESI –ve mode): m/z 351 (M-1)⁺; IR(KBr): 3066 cm⁻¹ (NH), 1684 cm⁻¹ (C=O). Elemental analysis for C₁₈H₁₂N₂O₆: Found: C, 60.89; H, 3.47; N, 7.63%; requires C, 61.37; H, 3.43; N, 7.95%.

10. *Isolated Yield 37%; MP: > 300 °C.* ¹H NMR(DMSO-*d*₆) δ : 7.07–7.11 (dd, 2H, *J* = 6.043, *J* = 3.022), 7.38–7.39 (d, 2H, *J* = 3.022), 8.23–8.26 (d, 2H, *J* = 8.309), 9.89 (s, 2H), 11.68 (s, 2H); MS (ESI –ve mode): m/z 483 (M-1)⁺; IR(KBr): 3250 cm⁻¹ (NH), 1672 cm⁻¹ (C=O). Elemental analysis for C₁₈H₁₂N₂O₈: Found: C, 55.92; H, 3.23; N, 6.91%; requires C, 56.25; H, 3.15; N, 7.29%.

Computational Studies. In this study, all of the calculations have been carried out using Gaussian 03 ab initio/DFT quantum chemical package.³⁴ The atomic positions of the molecules in all possible geometrical conformations were fully relaxed by Berny optimization algorithm at DFT-B3LYP with 6-311G(d,p) basis set with a default integration grid. The theoretical singlet/triplet equilibrium structures were obtained when the maximum internal forces acting on all the atoms and the stress were less than 4.5×10^{-4} eV/Å and 1.01×10^{-3} kbar respectively which were further confirmed by vibrational analysis. We carried out calculations of molecular properties with the B3LYP/6-311G(d,p) equilibrium minimal geometries. TDDFT (time dependent density functional theory) studies have been carried out to estimate the lowest 10 singlet–singlet transitions at the same basis set level both in vacuo and in solvent media (DMF).

Symmetry adapted cluster/symmetry adapted cluster configuration-interaction (SAC/SAC–CI) methods incorporated in Gaussian 03 package have been applied to many molecules and found to be quite accurate for studying molecular spectroscopy.^{12b,13a,35} The SAC method is based on the spin and space adapted formalism of the cluster expansion methods.^{35c} The SAC wave function is expanded as

$$|\Psi_{\text{SAC}}\rangle = \exp(s)|0\rangle$$

Where $s = \sum_i C_i S_i^\dagger$, $|0\rangle$ is the HF determinant and the operator S_i^\dagger is spin symmetry-adapted.

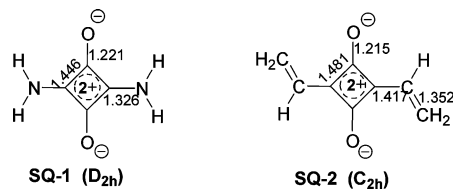


Figure 1. Model molecules: SQ-1 no diradical character (resonance structure as in Scheme 1b). SQ-2 having diradical character (resonance structure as in Scheme 1c). Bond lengths are given in Å.

Basically the SAC–CI is a cluster expansion method and it is usually more rapidly convergent than CI. SAC–CI methods take into consideration the singly and doubly excited states which mix up with the ground state and the targeted excited state. The SAC–CI wave function is written as

$$|\Psi_{\text{SAC-CI}}^p\rangle = R^p|\psi_{\text{SAC}}\rangle$$

where p represents the p th state and $R^p = \sum_k d_k^p R_k^\dagger$, R_k^\dagger represents a set of excitations, ionizations and d_k^p is the SAC–CI coefficient of p th excited state. Further details of this method are available in the literature.³⁵ We had applied this technique in our previous study of dyes based on the oxyallyl substructure with success (a difference of less than 0.1 eV with the experimental observed excitation energy was obtained), hence it is our choice for this study also.^{12b,13} In similar lines to our earlier study and literature reports by other researchers, the geometry of the model molecules in this work also have been optimized using the above-mentioned DFT methods and then subjected to SAC–CI.³⁶

For the ground state, SAC is carried out and is non variational, while for the excited state, SAC–CI is carried out using the variational methods. The active space is chosen with the window option where, depending on the molecule's size some core and some virtual molecular orbitals are not used in the active space. To the ground state, all the single excitation operators in this are also included without selection. For the doubles excitation operators an energy threshold value is used to select the configurations based on the perturbation method (vide infra). The SAC–CI is restricted to singles and doubles linked operators, while the higher order operators are treated through unlinked operators. All the single excitation operators in this are also included without selection. For the doubles excitation operators in both SAC and SAC–CI, estimated using the perturbation approach, there are three levels of selection. Those which contribute with a energy threshold (in Hartree) larger than 1.0×10^{-5} (SAC) and 1.0×10^{-6} (SAC–CI) is referred to as level one, those with 5.0×10^{-6} (SAC) and 5.0×10^{-7} (SAC–CI), as level two and those with 1.0×10^{-6} (SAC) and 1.0×10^{-7} (SAC–CI), as level three.

Results and Discussions

Model Molecules, SQ-1 and SQ-2. First we carry out computational studies on two model squaraine molecules namely SQ-1 and SQ-2 shown in Figure 1 and estimate the transition energies, diradical character, and NLO properties. The effect of a small diradical character on transition energies and NLO properties is illustrated through this calculation, or in other words the essential difference in the behavior of molecules having VB resonance structures as shown in Scheme 1b when compared to VB resonance structures in Scheme 1c is brought out.

Molecular Structures, Geometries, and Transition Energies of SQ-1 and SQ-2. SQ-1 has the donors (amine groups) attached directly to the SQ ring. Compared to SQ-1, SQ-2 has larger conjugation and there are no direct donor groups attached to the ring. There are two possible conformations for SQ-2 and for the discussion here we consider only the geometry which is slightly lower in energy ie the C_{2h} symmetry. We have shown earlier that the higher energy isomer (C_{2v}) of oxyallyl derivatives also have almost similar properties.^{13a} The geometry optimization to obtain the minimized geometry and the frequency analysis for confirming that it is minima are carried out. The geometry of the molecules (only bond lengths) are also given in Figure 1. The ground state dipole moments of these molecules are negligible. HOMO–LUMO gaps (HLG) are tabulated in Table 1. It is seen that the HLG of SQ-2 is much smaller than SQ-1.

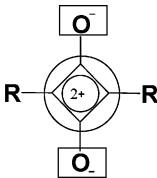
SAC–CI results are tabulated in Table 1. The ground to the lowest excited state transitions obtained from SAC–CI is 4.27 eV in SQ-1, and only 2.43 eV in SQ-2. The oscillator strengths indicate that these transitions are fairly intense. These results are in good agreement with the TD-DFT calculations which also predict 4.19 and 2.52 eV for SQ-1 and SQ-2 respectively. Charge transfer calculated (in e) using SAC–CI are shown in Table 2. Both O atoms act as withdrawing groups in the ground state and in the excited state as electron donors. In SQ-1 the O atoms in the ground state have a negative charge of -1.17 , whereas in SQ-2, the O atoms have a negative charge of -1.13 . The central rings carry a large positive charge of 1.32 in SQ-1 and only 0.76 in SQ-2 in the ground state. The ground state charges on R in both molecules are different. In SQ-1 it is -0.14 , whereas in SQ-2 it is 0.36 . In the excited state the negative charge decreases on the O atom in SQ-1 and now it is -0.93 , while similarly in SQ-2 it is now -0.85 . The central ring shows a decrease in the positive charge in SQ-1 by 0.21 , which indicates that it has accepted 0.21 charge in the excited state. Similar argument for SQ-2, indicates that the central ring has accepted 0.13 charge in the excited state. Interestingly in both molecules the larger charge donors are the oxygen atoms and the donation in both squaraines are almost similar, while, the side R groups act as acceptors in the excited state. In the case of SQ-1 the charge gained by the side group, R is very small ($0.04e$) while for SQ-2 it is $0.15e$. The central ring in both cases gain charge but it is relatively larger in SQ-1. Though there is larger charge transfer to central ring in SQ-1 but its absorption is blue-shifted when compared to SQ-2 by ~ 1.8 eV. Thus the nature of the absorption band is different in SQ-1 when compared to SQ-2. Gude and Rettig have reported negative solvatochromic effect in SQ-1 type of molecules.²⁷ Due to the lack of dipole in SQ-1 type of molecules they had attributed the solvatochromatic effect to the change in quadrupole moment.

Diradical Character of SQ-1 and SQ-2. Several methods have been suggested for estimating the diradical character. Wirz had suggested that a molecule can be said to be a diradical if the splitting between the singlet (S_0) and triplet (T_1) is around $2\text{--}24$ kcal/mol.³⁷ From this method one can see that SQ-2 due to its small singlet–triplet splittings can be considered as a diradicaloid (table 1). On the other hand the percent diradical character can also be estimated by using the method of occupation numbers.³⁸ Here it is related to the HOMO $-i$ and LUMO $+i$ and is defined as the weight of doubly excited

TABLE 1: Absorption Energies (ΔE in eV), Oscillator Strength (f), Transition Dipole Moments (μ_{ge} in Debye), Diradical Character (DRC), HOMO-LUMO Gap (HLG in eV), Singlet-Triplet Gap (ΔE_{S-T} in kcal/mol), and Second Hyperpolarizabilities (γ in esu) Obtained at HF-SAC/SAC-CI Level for the B3LYP/6-311G(d,p) Optimized Geometries of the Model Molecules

molecule	$\Delta E^{a,b}$	f	μ_{ge}	DRC ^c	HLG ^d	ΔE_{S-T}^e	γ in esu
SQ-1	4.27 (4.19)	0.397	1.95	0	10.24 (4.29)	53.38	-0.9×10^{-35}
SQ-2	2.43 (2.52)	0.344	2.35	27	7.67 (2.51)	18.24	-1.1×10^{-34}

^a HOMO-LUMO transitions are the major transitions. ^b In parentheses ΔE obtained from TDDFT calculations. ^c Diradical character (DRC) calculated at UHF/6-311G(d,p) level of theory. ^d HLG in parentheses obtained from DFT calculations. ^e ΔE_{S-T} obtained from B3LYP/6-311G(d,p) optimized geometries.

TABLE 2: Charge Transfer from Ground to Excited States of Model Molecules Obtained at SAC (Ground State) and SAC-CI (Excited State) Level of Theory


molecule	group	ground state charge	excited state charge	gain/loss ^a
SQ-1	I	-1.17	-0.93	-0.25
	II	1.32	1.11	0.21
	III	-0.14	-0.18	0.04
SQ-2	I	-1.13	-0.85	-0.27
	II	0.76	0.64	0.13
	III	0.36	0.22	0.14

^a Represents the gain/loss of electron charge density (in e) in the respective groups, upon excitation of the molecule from ground to excited state. Loss is shown as a negative sign.

configuration in the MC-SCF theory and is formally expressed in the spin-projected UHF (PUHF) theory as³⁹

$$\text{DRC} = \left(1 - \frac{2S_i}{1 + S_i^2}\right) \times 100 \quad (1)$$

where S_i is the orbital overlap ($\chi_{\text{HOMO}-i}$ and $\eta_{\text{HOMO}-i}$) between the corresponding pairs

$$\chi_{\text{HOMO}-i} = \cos(\omega)\phi_{\text{HOMO}-i} + \sin(\omega)\phi_{\text{LUMO}+i} \quad (2)$$

and

$$\eta_{\text{HOMO}-i} = \cos(\omega)\phi_{\text{HOMO}-i} - \sin(\omega)\phi_{\text{LUMO}+i} \quad (3)$$

Here ω and ϕ represent the UHF natural orbital (UNO) and orbital mixing parameter, respectively. The orbital overlap can be replaced by the occupation numbers (n_i) of UNOs, which are obtained from the density matrix. This has been shown to be suitable.^{29c} Therefore S_i can be expressed as

$$S_i = \frac{n_{\text{HOMO}-i} - n_{\text{LUMO}+i}}{2} \quad (4)$$

The singlet-triplet gap and the calculated DRC are shown in Table 1. The singlet-triplet gap is large in SQ-1 (53.38 kcal/mol) while in SQ-2 it is much smaller (18.24). The calculated

DRC for both SQ-1 and SQ-2 are in agreement with the singlet-triplet gap: SQ-1 has zero diradical character, while SQ-2 has around 27%. The reason for SQ-2 having a larger DRC than SQ-1 can be explained as follows. On increasing the conjugation in SQ-2, the HLG narrows thus enhancing the open shell character.

Second Hyperpolarizability of SQ-1 and SQ-2. When a molecule is exposed to a medium with an optical electric field, it becomes polarized. At the microscopic level, the response can be expressed as a function of dipole and energy as⁵

$$\mu_i(F) = \mu_i(0) + \alpha_{ij}F_j + \frac{1}{2}\beta_{ijk}F_jF_k + \frac{1}{6}\gamma_{ijkl}F_jF_kF_l + \dots \quad (5)$$

$$E(F) = E(0) - \mu_iF_i - \frac{1}{2}\alpha_{ij}F_iF_j - \frac{1}{6}\beta_{ijk}F_iF_jF_k - \frac{1}{24}\gamma_{ijkl}F_iF_jF_kF_l + \dots \quad (6)$$

where $\mu_i(0)$, is its permanent dipole, $E(0)$ is the energy of molecule in the absence of electric field, α_{ij} is the dipole polarizability, and β_{ijk} and γ_{ijkl} are first and second hyperpolarizability tensors respectively obtained as first, second, third order derivatives of dipole moment μ_i with respect to the applied field F ; that is, the n th order polarizability can be expressed as the n th-order derivative of dipole moment or the $(n+1)$ th derivative of the total energy since the dipole moment is the negative first order derivative of molecular total energy.

$$\alpha_{ij} = \left(\frac{\partial \mu_i}{\partial F_j}\right)_{F=0} \quad (7)$$

$$\beta_{ijk} = \left(\frac{\partial^2 \mu_i}{\partial F_j \partial F_k}\right)_{F=0} \quad (8)$$

$$\gamma_{ijkl} = \left(\frac{\partial^3 \mu_i}{\partial F_j \partial F_k \partial F_l}\right)_{F=0} \quad (9)$$

Basically there are two commonly used techniques to calculate the polarizabilities. The first one is the sum-overstates (SOS) method and the other is finite-field (FF) method.

SOS Method. In this section we briefly describe the structure-property correlation based on the perturbative treatment. The equation for γ can be written as^{5,40}

$$\gamma_{iii} = 24 \sum_{n \neq g} \left[\frac{(\mu_{ng}^i \Delta \mu_{ng}^i)^2}{(E_{ng})^3} - \frac{(\mu_{ng}^i)^4}{(E_{ng})^3} + \sum_{m \neq n, g} \frac{(\mu_{ng}^i)(\mu_{nm}^i)^2}{(E_{ng})^2 E_{mg}} \right]$$

and

$$\gamma_{ijj} = 4 \sum_{n \neq g} \left[\frac{4\mu_{ng}^i \mu_{ng}^j \Delta \mu_{ng}^i \Delta \mu_{ng}^j + (\mu_{ng}^i \Delta \mu_{ng}^j)^2 + (\mu_{ng}^j \Delta \mu_{ng}^i)^2}{(E_{ng})^3} - \frac{6(\mu_{ng}^i \mu_{ng}^j)^2}{(E_{ng})^3} + \sum_{m \neq n, g} \frac{4\mu_{ng}^i \mu_{nm}^i \mu_{ng}^j \mu_{nm}^j + (\mu_{ng}^i \mu_{nm}^j)^2 + (\mu_{ng}^j \mu_{nm}^i)^2}{(E_{ng})^2 E_{mg}} \right]$$

where $i = x, y, z$ (10)

Here the parameters μ_{ng} and μ_{nm} , correspond to the transition moments between the ground and the n th excited state and n th excited to m th excited states. $\Delta \mu_{ng}$ is the difference in dipole moments between the ground and the n th excited states. Similarly E_{ng} and E_{mg} correspond to the energy of transition between the ground and the n /mth excited state.

In the three state model approximation [ground (A),⁴⁰ excited state (B), and the final state (A)] and using the symmetry arguments like $\Delta \mu_{ng}^y$ is zero and transition dipole moments in Z being zero and X very small, we obtain only the following longitudinal major component for our case here:

$$\gamma_{yyyy} = 24 \sum_{n \neq g} \left[-\frac{(\mu_{1B_2, 1A_1}^y)^4}{(E_{1B_2, 1A_1})^3} + \sum_{m \neq n, g} \frac{(\mu_{1B_2, 1A_1}^y)(\mu_{2A_1, 1B_2}^y)^2}{(E_{1B_2, 1A_1})^2 E_{2A_1, 1B_2}} \right] \quad (11)$$

or in other words $\gamma^T = \gamma^2 + \gamma^3$ where the first term in equation 11 is γ^2 and the positive term is γ^3 . In the above expression if the first term dominates, then a negative value is obtained and if second term dominates, a positive value is obtained. From the equation it is also clear that when the transition dipole moment is large and the transition energy is small the γ^2 value increases.

SOS three state method has been used earlier by other workers to understand the transitions responsible for the origin of γ in molecules.^{9,40a} We use this SOS three state model here for understanding the second order hyperpolarizability of SQ-1 and SQ-2 systems. It has been suggested based on the experimental observations that in the case of SQ dyes only γ^2 term is the dominant term.^{18d} Hence we estimate the third order NLO property of these two molecules by calculating only the dominant term. The γ values are shown in Table 1. It is seen that the γ value of SQ-2 is larger than SQ-1 by almost an order of magnitude.

From the above computational results obtained for the two squaraines SQ-1 and SQ-2, it is clear that the SQ-1 can be represented by the resonance structure in Scheme 1b, while SQ-2 can be represented by Scheme 1c. Thus the red shift in absorption seen in, SQ-2 compared to SQ-1 and the nearly order of magnitude larger γ value obtained for the former molecule when compared to latter can be attributed to the larger diradical character.^{9,41} In other words the CT in SQ-1 is largely responsible for the absorption, and in SQ-2 the absorption is due to the diradical character. The SQ-1 can be classified as a D-A-D type of molecule based on experiments reported earlier and the CT observed using SAC-CI. In this study our interest is to investigate SQ-1 type of molecules experimentally (derivatives **1–10**). Comparison of the transition energies obtained by SAC-CI and TDDFT methods are also shown in Table 1. The TDDFT almost reproduces the values obtained by the high level SAC-CI methodologies for these type of molecules (**1–10**).

Molecular Structures and Geometries of 1–10. As our main aim is determining the molecular NLO property γ and its variation with substitutions in **1–10**, it would be of interest to predict the conformations and geometry of the molecules in gas phase using quantum chemical methods. We can broadly classify the molecules into two subgroups, one which have donating/accepting groups at the o or p positions of the aminophenyl group and other which do not. The first six molecules belong to the latter class while the last four belong to the former class. We notice that there are many possible planar conformations for the molecules **7** and **10** unlike the others which have only two low lying major conformations. The calculated energies of these conformations reveal that all the low lying have very small energy difference between each other. The details of the geometrical parameters of the central ring of all the molecules, their conformations and relative energies obtained at the B3LYP/6-311G (d, p) level are indicated in the Figure 2 and Figure A (Supporting Information). The bond lengths show a large variation in the ring.

From the Figure A (Supporting Information) it is clearly seen that the relative energy differences for all of the molecules in the gas phase between conformations are very small. We have also carried out the calculation of the relative energies in the solvent phase (single point). The relative energy differences for all the molecules in the solvent phase between conformations now decreases. In Table 3 the singlet–triplet splitting is given, which is very large. This indicates that these do not have any singlet diradical character. This is further supported by the DRC values calculated using the methodology given earlier for all the molecules which turn out to be zero. The HLG (B3LYP) given in the same table range from 2.96 to 3.45 eV).

Solid State Properties of 1–10. At room temperature, **1–10** are solids. The solid-state properties of these such as melting point, thermal stability (TGA analysis) were determined and the corresponding TGA data and melting point data are presented in Table 4. The TGA analysis shows that the thermal decomposition range is 294–455 °C. This high thermal stability indicates that these will be quite stable in the incident laser environment, i.e., there will not be any damage to the material by the impact of the laser light.

Electronic Absorption Spectrum (Linear Optical Properties) of 1–10. We have carried out the UV–visible absorption spectrum analysis of **1–10** in DMF. The obtained spectra are shown in Figure 3. The range of absorption is 387 to 442 nm with the variation attributed to the substitution effect. There is no absorption at 800 nm (laser wavelength for NLO studies), which is seen zooming the region at 800 nm. Systematic solvatochromic studies could not be carried out as these have little solubility in nonpolar solvents. None of these compounds show any detectable fluorescence at room temperature when excited hence no fluorescence data is reported. **1–6** show almost identical single intense bands in which the λ_{\max} varies slightly due to different substitutions. In **7** and **10** we see the band with two peaks/shoulder.

To have a deeper understanding of the observed spectra, we have carried out TDDFT studies including the solvent effect of these molecules and their various conformational isomers. The values obtained are tabulated in Table 5. The major transitions at the orbital level in all the molecules are observed to be HOMO–LUMO, which is localized on the central ring. The MO picture for all the molecules is shown in Figure B (Supporting Information). From the TDDFT studies of the lowest conformations we observe that only the intense band with a single peak can be assigned in all molecules. Thus the

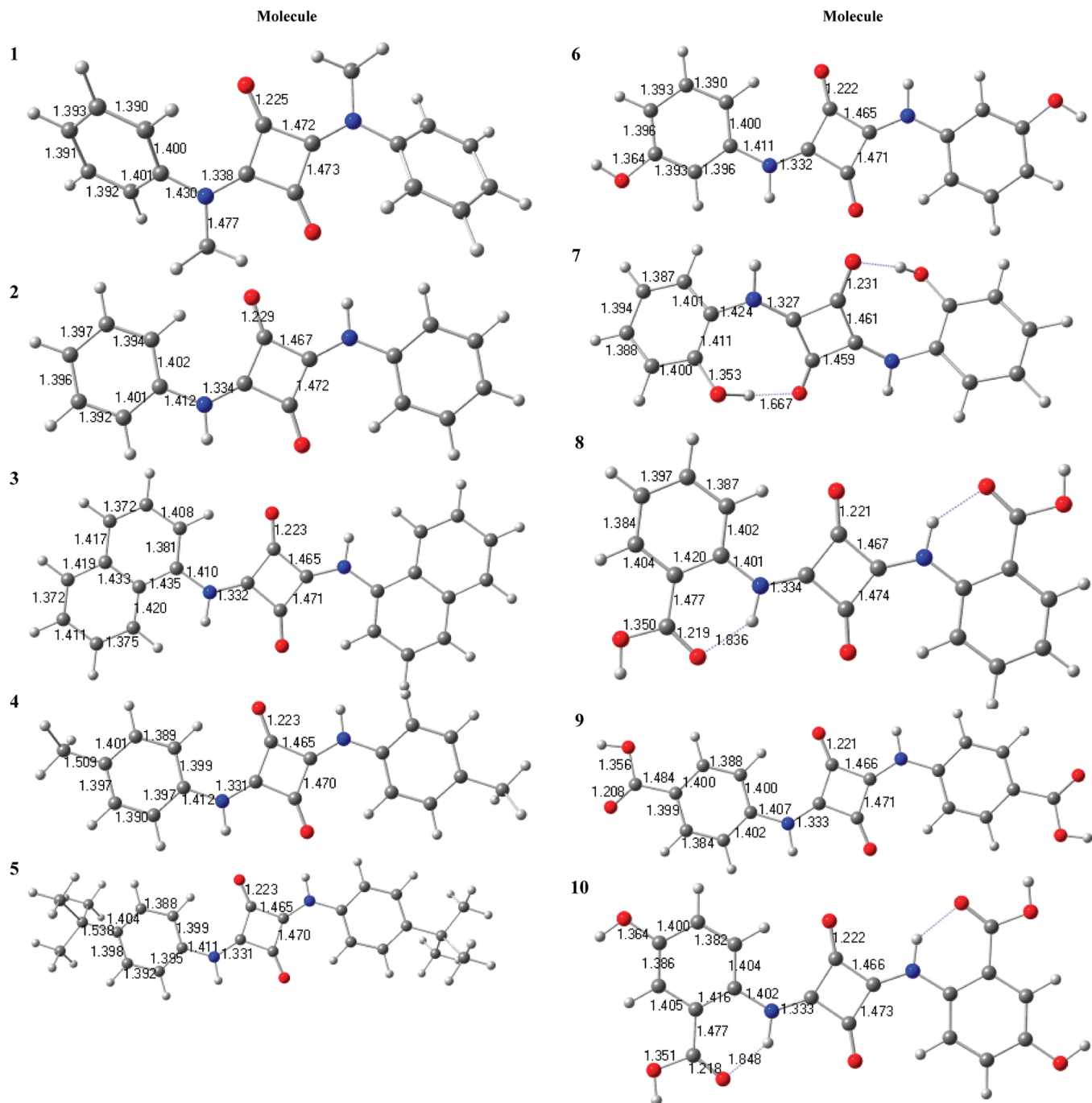


Figure 2. Geometrical parameters (bond lengths in Å) for the lowest energy conformations of **1–10**, calculated at B3LYP/6-311G(d,p) level of theory.

TABLE 3: HOMO-LUMO Gap (HLG in eV), Singlet-Triplet Gap (ΔE_{S-T} in kcal/mol) of **1–10 at B3LYP/6-311G(d,p) Level of Theory**

molecule	HLG	ΔE_{S-T}
1	3.45	41.3
2	3.39	43.7
3	3.07	40.4
4	3.36	43.7
5	3.36	43.7
6	3.40	44.0
7	3.30	42.9
8	3.08	40.8
9	3.20	42.2
10	2.96	40.2

TABLE 4: Solid State Properties of **1–10**

molecule	mp °C	TGA °C
1	183–186	294
2	>300	421
3	>300	378
4	>300	403
5	>300	417
6	>300	400
7	279–283	373
8	>300	352
9	>300	455
10	>300	377

double peak/shoulder in **7** and **10** is not due to the monomeric neutral species.

To understand the origin of the second peak/shoulder, we carryout further spectroscopic investigations. In the literature such a double peak has been assigned to aggregation/or water

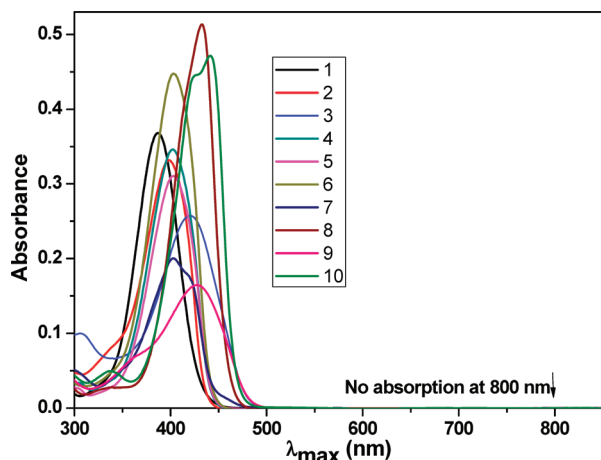


Figure 3. UV-visible absorption spectra of 1–10 in DMF.

TABLE 5: Experimental Absorption Maxima (λ_{max} in nm), Calculated Absorption Energies (ΔE in eV), Oscillator Strength (f), and Transition Dipole Moments (μ_{gc} in Debye) of 1–10 in Dimethylformamide (DMF) Obtained at TDDFT-B3LYP/6-311G(d,p) Level

mol.	λ_{max} in nm ^a	ΔE^b	f	μ_{gc}^c
1	387 (4.46)	3.19 (389)	0.869	8.48
2	399 (4.28)	3.17 (391)	1.182	9.91
3	420 (3.65)	2.78 (446)	1.170	10.54
4	403 (5.74)	3.15 (394)	1.326	10.54
5	404 (5.73)	3.14 (395)	1.451	11.04
6	404 (4.99)	3.19 (389)	1.143	9.73
7	403 (2.05)	3.06 (405)	1.194	10.15
8	433 (7.16)	2.88 (431)	1.070	9.90
9	428 (3.39)	2.93 (423)	1.414	11.29
10	442 (7.05)	2.74 (453)	1.121	10.39

^a In parentheses ($\epsilon \times 10^4 \text{ M}^{-1} \text{ cm}^{-1}$). ^b In parentheses λ_{max} in nm.

^c Transitions in 1–10 are HOMO–LUMO transitions, having CI coefficient larger than 0.64.

induced aggregation.⁴² Some other recent studies have shown that in some cases it could also arise due to traces of water present in the organic solvent interacting with the dye which leads to acid–base equilibrium and not aggregation.^{33a,43}

We first carried out the UV–visible absorption studies at different concentrations of all the dyes in pure DMF (1×10^{-6} – $16 \times 10^{-6} \text{ M}$). In case aggregation takes place, we should expect a change in the two peaks intensities relative to each other with increasing amount of the solute.⁴² The peaks (shown in Figure 4a for 1 and 4b for 10 and the rest in Supporting Information Figure C) do not change their relative intensity, thus ruling out aggregation. We then compare the effect of addition of water (shown in panels a and b of Figure 5) for 1 and 10. With increasing volume of water in the solvent from 300 μL to 1 mL we notice that there is no shift in the λ_{max} for 10. But slowly and progressively the intensity of the second peak increases with increasing water concentration. On addition of 1 mL of water we notice that the intensities of the two peaks are reversed. Any further addition of water, blue shifts the entire band. In the case of 1 (Figure 5a) we notice that there is no change in the intensity of the band or no new bands are formed with increasing water in the solvent. When the water content is almost 50% in the solvent then the band blue shifts in this case also. This clearly suggests, here 7 and 10 undergo acid base equilibrium and not aggregation.^{33a,43}

Charge transfer calculated using SAC/SAC–CI is shown in Table 6 for all of the molecules. In the ground state the central

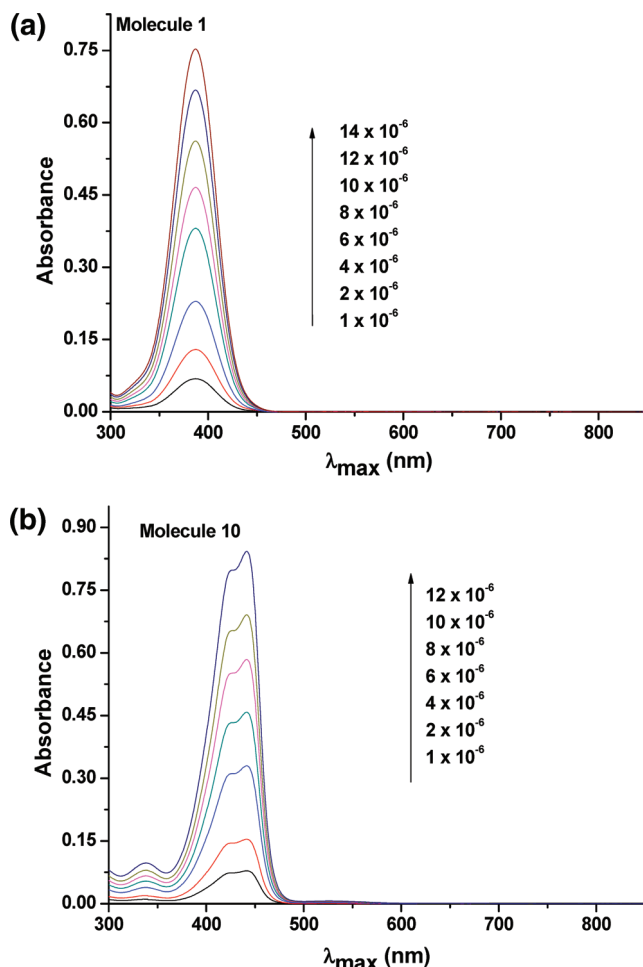


Figure 4. (a) UV–visible absorption spectra of 1 in DMF at various concentrations. (b) UV–visible absorption spectra of 10 in DMF at various concentrations.

ring has around 1.43–1.49 positive charge in all the molecules. This is quite close to ideal positive charge as represented in Scheme 1a. The O atoms (both together) have charges ranging from -0.21 to -0.28 . On excitation, interestingly the amino groups are larger charge donors than the oxygens except in 8. The donation from the O atoms ranges from 0.04 to 0.10, which compared to SQ-1 and SQ-2 is greatly reduced. Charge transfer to the central accepting ring varies from 0.12 to 0.20e. As these have no diradical character these molecules are purely SQ-1 type molecules.

Third Order Nonlinear Optical Studies of 1–10. The third order NLO, $\chi^{(3)}$ is obtained by comparing the measured DFWM signal for the sample with that of DMF as reference ($\chi^{(3)} = 4.4 \times 10^{-14} \text{ esu}$) under the same experimental conditions and the DMF $\chi^{(3)}$ is estimated by using CCl_4 as standard ($\chi^{(3)}$ of CCl_4 is $1.35 \times 10^{-14} \text{ esu}$). The following relationship is used.

$$\chi^{(3)}_{\text{sample}} = \left(\frac{n_{\text{sample}}}{n_{\text{ref}}} \right)^2 \left(\frac{I_{\text{sample}}}{I_{\text{ref}}} \right)^{1/2} \left(\frac{L_{\text{ref}}}{L_{\text{sample}}} \right) \alpha L_{\text{sample}} \times \left(\frac{e^{\alpha L_{\text{sample}}/2}}{1 - e^{-\alpha L_{\text{sample}}}} \right) \chi_{\text{ref}}^{(3)} \quad (12)$$

where I is the DFWM signal intensity, α is the linear absorption coefficient, L is sample path length, and n is the refractive index. The concentration of sample is very low in solution, so we have taken the refractive index of DMF ($n = 1.431$) as the refractive

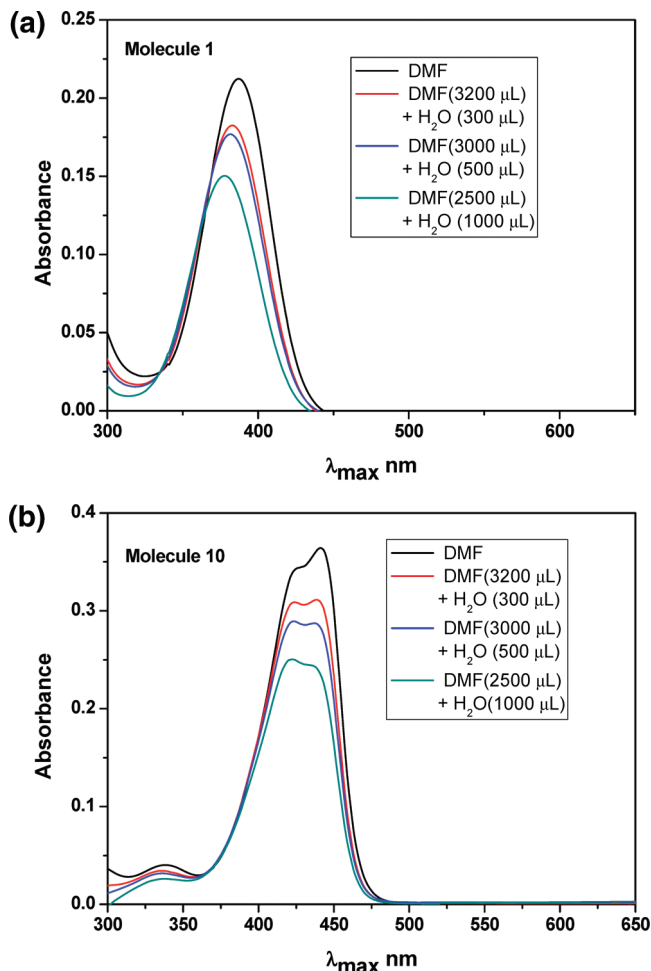


Figure 5. a: UV-visible absorption spectra of 1 in DMF with addition of water. Figure 5b: UV-visible absorption spectra of 10 in DMF with addition of water.

index of solution. The $\chi^{(3)}$ is estimated in DMF at concentration 1×10^{-4} M. The $\chi^{(3)}$ values at this concentration are tabulated in Table 7. $\chi^{(3)}$ has three independent components namely $\chi_{111}^{(3)}$, $\chi_{1212}^{(3)}$, and $\chi_{1221}^{(3)}$ in an isotropic medium. In the case of nonresonant electronic NLO, $\chi_{111}^{(3)} = 3\chi_{1212}^{(3)} = 3\chi_{1221}^{(3)}$ when the three input beams are all vertically polarized, then the corresponding $\chi^{(3)}$ obtained would be $\chi_{111}^{(3)}$. To determine $\chi_{1212}^{(3)}$, the probe beam is orthogonally polarized with respect to the two pump beams. The ratio of $\chi_{111}^{(3)}$ to $\chi_{1212}^{(3)}$ should be close to 3 (suggesting that there is no significant contribution arising from the coherent coupling effects).⁴⁴ Here for all samples we obtain values close to 3 (2.71 to 3.13). Since these molecules absorb around 400 nm, it is expected to have a contribution for two photon absorption. In order to rule out the contribution of two-photon absorption to the measured values of $\chi^{(3)}$, we carried out the nonlinear transmittance measurements and the input intensity dependent study of the obtained DFWM signal. To study the nonlinear transmittance, we carried out the open aperture Gaussian beam Z-scan^{45a} study for all these samples. Figure 6a shows the Z scan curves indicating the reverse saturable absorption nature. In order to estimate whether two photon absorption (2PA) or three photon absorption (3PA) is dominating, the experimental data is fitted using the formalism developed in ref 45 with the transmittance given as⁴⁵

$$T_{\text{OA}(n\text{PA})} = 1 - \frac{\alpha_n I_0^{n-1} L_{\text{eff}}^{(n)}}{n^{3/2} (1 + z^2/z_0^2)^{n-1}} \quad (13)$$

$$T_{\text{OA}(2\text{PA})} = 1 - \frac{\alpha_2 I_0 L_{\text{eff}}}{2^{3/2} (1 + z^2/z_0^2)} \quad (14)$$

$$T_{\text{OA}(3\text{PA})} = 1 - \frac{\alpha_3 I_0^2 L_{\text{eff}}'}{3^{3/2} (1 + z^2/z_0^2)^2} \quad (15)$$

where I_0 is the peak intensity, z is the sample position, $z_0 = \pi\omega_0^2/\lambda$ is Rayleigh range, ω_0 is the beam waist at the focal point ($z = 0$), λ is the laser wavelength, and effective path lengths in the sample of length $L_{\text{eff}}^{(n)}$ for 2PA and 3PA are given as $L_{\text{eff}} = [1 - \exp(-\alpha_0 L)]/\alpha_0$, and $L_{\text{eff}}' = [1 - \exp(-2\alpha_0 L)]/2\alpha_0$, respectively. α_2 and α_3 represent nonlinear absorption coef-

TABLE 6: Charge Transfer from Ground to Excited States of 1–10 Obtained at SAC (Ground State) and SAC–CI (Excited State) Level of Theory

molecule	group	ground state charge	excited state charge	gain/loss ^a
1	I	-1.22	-1.15	-0.07
	II	1.43	1.31	0.12
	III	-0.21	-0.16	-0.05
2	I	-1.21	-1.16	-0.05
	II	1.46	1.29	0.17
	III	-0.24	-0.13	-0.12
3	I	-1.22	-1.17	-0.04
	II	1.48	1.29	0.19
	III	-0.26	-0.11	-0.15
4	I	-1.20	-1.16	-0.04
	II	1.44	1.28	0.16
	III	-0.24	-0.12	-0.12
5	I	-1.21	-1.15	-0.06
	II	1.45	1.25	0.20
	III	-0.24	-0.10	-0.14
6	I	-1.20	-1.14	-0.06
	II	1.46	1.29	0.17
	III	-0.26	-0.15	-0.11
7	I	-1.20	-1.16	-0.04
	II	1.44	1.28	0.16
	III	-0.24	-0.12	-0.12
8	I	-1.21	-1.13	-0.08
	II	1.48	1.35	0.14
	III	-0.27	-0.22	-0.05
9	I	-1.21	-1.11	-0.10
	II	1.49	1.30	0.18
	III	-0.28	-0.20	-0.08
10	I	-1.21	-1.13	-0.08
	II	1.48	1.31	0.17
	III	-0.26	-0.18	-0.09

^a Represents the gain/loss of electron charge density (in e) in the respective groups, upon excitation of the molecule from ground to excited state. Loss is shown as negative sign.

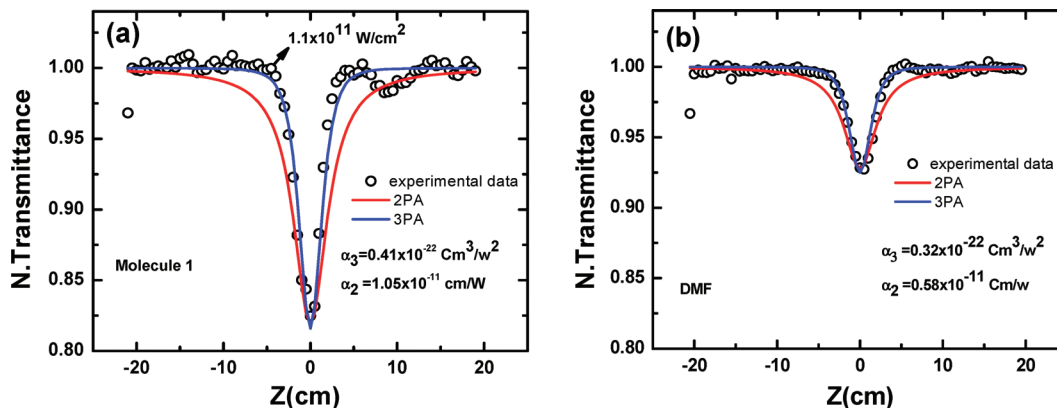


Figure 6. Z-scan open aperture studies for the solvent DMF and **1**.

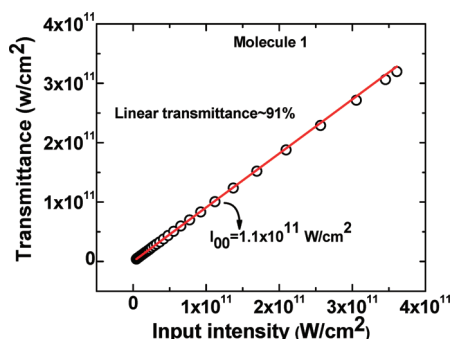


Figure 7. Plot of output transmittance vs input power for **1**.

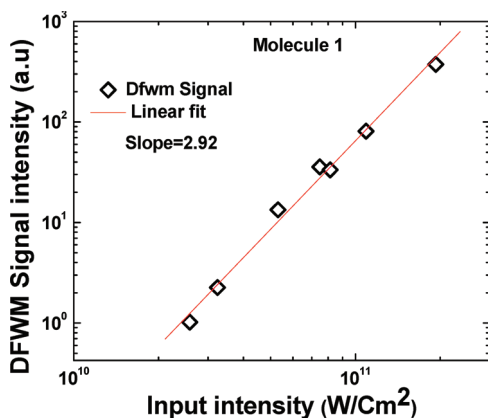


Figure 8. Plots showing the cubic dependence of DFWM as a function of input intensity for **1**.

ficients for 2PA (two photon absorption) and 3PA (three photon absorption), respectively. Z-scan traces are fitted, using the eqs 14 and 15. The red line assumes 2PA and the blue line 3PA process. We can see that the best fit, given by the blue line in Figure 6a, is obtained with 3PA coefficient α_3 ($0.41 \times 10^{-22} \text{ cm}^3/\text{W}^2$) and the red line is obtained with 2PA coefficient α_2 ($1.05 \times 10^{-11} \text{ cm/W}$) having little contribution. To confirm if the three photon absorption is due to the solute molecule or the solvent DMF, we recorded nonlinear transmittance due to the pure solvent alone shown in Figure 6b. By comparing this data with the sample solution, we conclude that major contribution comes from the solvent and not the solute.

The DFWM signal was measured at $1.1 \times 10^{11} \text{ W/cm}^2$, which is well below the appearance of nonlinear absorption. In Figure 7, we show the transmission as a function of the input intensity for a range of intensities from 7×10^{10} until $4 \times 10^{11} \text{ W/cm}^2$

for **1** and others are shown in the Supporting Information (Figure D). From Figures 3 and 7, we can conclude that the linear absorption is negligible and that there is no two photon absorption in these molecules. DFWM signal is recorded and is shown in Figure 8 for different input intensities. From Figure 8, recorded for **1** and others in the Supporting Information (Figure E), we obtained a slope of ~ 3 for all of the samples studied indicating that origin of DFWM does not have contribution from any two-photon absorption in which case the slope of the curve would have been higher than 3.

The $\chi^{(3)}$ values vary from 3.5×10^{-14} to $3.9 \times 10^{-14} \text{ esu}$, and are quite large as shown in Table 7. The temporal response of **1** is shown in Figure 9. The nonlinear responses are very fast and are of the order of 100 fs or faster (for other molecules see Supporting Information Figure F).

The second order hyperpolarizability (γ) is obtained from the $\chi^{(3)}$ of the sample by the following equation:

$$\chi_{\text{sample}}^{(3)} = \left(\frac{n^2 + 2}{3} \right)^4 [N_{\text{solvent}} \gamma_{\text{solvent}} + N_{\text{sample}} \gamma_{\text{sample}}] \quad (16)$$

Here the term T is a local field factor, i.e., $(n^2 + 2)/3 = T$, where n is the refractive index, N_0 is the number density, and γ is the second hyperpolarizability. The Number density N_0 is related to the Avogadro number and concentration of solution (C_s) as

$$N_0 = NC_s/1000 \quad (17)$$

We carried out the determination of $\chi^{(3)}$ as a function of concentration (1×10^{-3} to $10 \times 10^{-4} \text{ M}$) for **3**. We see from the plots for $\chi^{(3)}$ vs concentration a linear decrease with a negative slope as shown in Figure 10 (decreasing $\chi^{(3)}$ with increasing solute concentration) indicates that the γ value would be of opposite sign with respect to the solvent. The experimentally determined γ values are large and vary from -1.2 to $-6.8 \times 10^{-33} \text{ esu}$ as shown in Table 7 (The values obtained for **7** and **10** may not be due to a single species (vide supra) as the experiments have been conducted in DMF.)

To understand the factors responsible for the large γ value we carry out theoretical analysis of these molecules using quantum chemical methods. It should be kept in mind that our aim is not to determine total γ through computational methods but we are only looking at the component originating due to

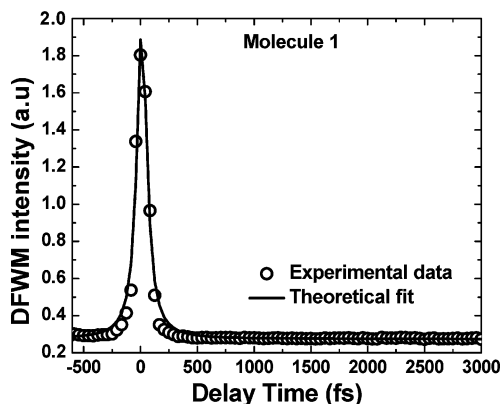


Figure 9. Temporal profile of DFWM signal of 1 in DMF (concentration: 1×10^{-4} M) as a function of beam 3 delay time for the parallel configurations.

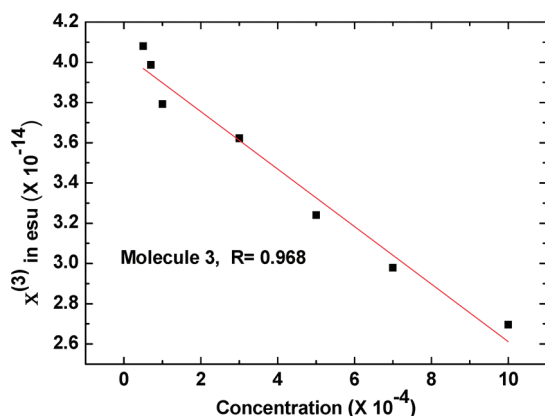


Figure 10. Plot of concentration dependence on $\chi^{(3)}$ for 3.

TABLE 7: Measured Third-Order Nonlinear Susceptibility ($\chi^{(3)}$ in esu), Second Order Hyperpolarizability (γ_{obs} in esu) of 1–10, Obtained from DFWM Technique in DMF^a

molecules	experimental		theoretical	
	$\chi^{(3)} \times 10^{-14}$	$\gamma_{\text{obs}} \times 10^{-33}$	gas phase $\gamma_{\text{calc}} \times 10^{-33}$	DMF $\gamma_{\text{calc}} \times 10^{-33}$
1	3.8	−5.9	−0.09	−0.2
2	3.7	−5.3	−0.2	−0.4
3	3.9	−2.6	−0.5	−0.7
4	3.9	−5.5	−0.3	−0.5
5	3.8	−4.8	−0.4	−0.6
6	3.7	−5.9	−0.2	−0.3
7	3.9	−1.2	−0.3	−0.4
8	3.9	−2.8	−0.3	−0.5
9	3.6	−6.8	−0.5	−0.8
10	3.5	−3.9	−0.4	−0.7

^a Also given are the calculated second order hyperpolarizability (γ_{calc} in esu) using two state model at the TDDFT-B3LYP/6-311G(d,p) level.

the central oxyallyl ring. The rest of the γ which we are not calculating originates from the side groups and higher states.

We evaluated the γ for each molecule using the transition dipole moment and the excitation energy obtained in DMF by TDDFT. These are also tabulated in Table 7. The γ is also very large (-0.1 to -0.5×10^{-33} esu in gas phase and -0.2 to -0.8×10^{-33} esu in DMF solvent) indicating that this central ring in each molecule contributes a large value to the total γ .

Conclusions

The synthesized squaraines 1–10 have a high stability as determined by TGA studies and also absorption in the region less than 500 nm. The DRC determined by computational methods show that these have no diradical character. The charge transfer from the side groups and the oxygen atom to the central ring as seen in the molecules and from the earlier experiments on the parent molecule points to the largely D-A-D nature in these molecules. The nonresonant NLO activity (γ) is determined using DFWM techniques at 800 nm. We obtain large $\chi^{(3)}$ values in DMF, and ultrafast optical response is also observed. We also determined the γ values in the solvent and find them to be very large in magnitude and negative in sign. These values are slightly smaller than the γ values of the more common squaraines absorbing above 600 nm reported in the literature. This decrease in γ is attributed to the lack of diradical character in these molecules. The large γ values and tunable absorption maxima indicates that these dyes are promising molecular materials.

Acknowledgment. We are thankful to DST, New Delhi for the funding of this project. We are also very much thankful to The Director, IICT and to The Head, Inorganic chemistry Division, IICT for their constant support in this work. ChP thanks CSIR for the fellowship and DNR thanks DST for financial support of project.

Supporting Information Available: Additional figures. This material is available free of charge via the Internet at <http://pubs.acs.org>.

References and Notes

- (1) *Introduction to Nonlinear Optical Effects in Molecules and Polymers*; Prasad, P. N., Williams, D. J., Eds.; Wiley: New York, 1991.
- (2) *Conjugated Polymers: The Novel Science and Technology of Highly Conducting and Nonlinear Optically Active materials*; Bredas, J. L., Silbey, R. J., Eds.; Kluwer: Dordrecht, Netherlands, 1991.
- (3) *Nonlinear Optical Materials. Theory and Modeling*; Karna, S. P., Yeates, A. T., Eds.; ACS Symposium Series 628; American Chemical Society: Washington, DC, 1996.
- (4) (a) Kanis, D. R.; Ratner, M. A.; Marks, T. J. *Chem. Rev.* **1994**, *94*, 195. (b) Zyss, J.; Ledoux, I. *Chem. Rev.* **1994**, *94*, 77. (c) Williams, D. J. *Angew. Chem., Int. Ed. Engl.* **1984**, *23*, 690.
- (5) Bredas, J. L.; Adant, C.; Tackx, P.; Persoons, A.; Pierce, B. M. *Chem. Rev.* **1994**, *94*, 243, and references cited therein.
- (6) (a) *Molecular Nonlinear Optics: Materials, Physics, and Devices*; Zyss, J., Ed.; Academic Press: Boston, 1993. (b) Sutherland, R. L. *Handbook of Nonlinear Optics*; Dekker: New York, 1996. (c) Lindsay, G. A. Singer, K. D. in *Polymers for Second-Order Nonlinear Optics*; ACS Symposium Series 601; American Chemical Society: Washington, DC, 1995.
- (7) (a) Verbiest, T.; Houbrechts, S.; Kauranen, M.; Clays, K.; Persoons, A. *J. Mater. Chem.* **1997**, *7*, 2175. (b) Verbiest, T.; Clays, K.; Samyn, C.; Wolff, J.; Reinholdt, D.; Persoons, A. *J. Am. Chem. Soc.* **1994**, *116*, 9320. (c) Bredas, J. L.; Meyers, F.; Pierce, B. M.; Zyss, J. *J. Am. Chem. Soc.* **1992**, *114*, 4928. (d) Verbiest, T.; Clays, K.; Persoons, A.; Meyers, F.; Bredas, J. L. *Opt. Lett.* **1993**, *18*, 525.
- (8) (a) *Nonlinear Optical Properties of Organic Molecules and Crystals*; Chemla, D. S., Zyss, J., Eds.; Academic Press: Orlando, FL, 1987; Vols. 1 and 2. (b) *Nonlinear Opt.*; Boyd, R. W., Ed.; Academic Press: New York, 1992.
- (9) Nakano, M.; Kishi, R.; Ohta, S.; Takebe, A.; Takahashi, H.; Furukawa, S.; Takashi, K.; Morita, Y.; Nakasuiji, K.; Yamaguchi, K.; Kamada, K.; Ohta, K.; Champagne, B.; Botek, E. *J. Chem. Phys.* **2006**, *125*, 74113.
- (10) (a) Nakano, M.; Takashi, K.; Kamada, K.; Ohta, K.; Kishi, R.; Ohta, S.; Nakagawa, N.; Takahashi, H.; Furukawa, S.; Morita, Y.; Nakasuiji, K.; Yamaguchi, K. *Chem. Phys. Lett.* **2006**, *418*, 142. (b) Ohta, S.; Nakano, M.; Takashi, K.; Kamada, K.; Ohta, K.; Kishi, R.; Nakagawa, N.; Champagne, B.; Botek, E.; Umezaki, S.; Takebe, A.; Takahashi, H.; Furukawa, S.; Morita, Y.; Nakasuiji, K.; Yamaguchi, K. *Chem. Phys. Lett.* **2006**, *420*, 432. (c) Nakano, M.; Nakagawa, N.; Ohta, S.; Kishi, R.; Takashi, K.; Kamada, K.; Ohta, K.; Champagne, B.; Botek, E.; Takahashi, H.; Furukawa, S.; Morita, Y.; Nakasuiji, K.; Yamaguchi, K. *Chem. Phys. Lett.*

- 2006, 429, 174. (d) Nakano, M.; Nagai, H.; Fukui, H.; Yoneda, K.; Kishi, R.; Takahashi, H.; Shimizu, A.; Kubo, T.; Kamada, K.; Ohta, K.; Champagne, B.; Botek, E. *Chem. Phys. Lett.* **2008**, *467*, 120. (e) Kubota, K.; Takahashi, H.; Fukui, H.; Bonness, S.; Yoneda, K.; Kishi, R.; Kamada, K.; Kubo, T.; Ohta, K.; Champagne, B.; Botek, E.; Nakano, M. *Chem. Phys. Lett.* **2009**, *477*, 309. (f) Nagai, H.; Nakano, M.; Yoneda, K.; Fukui, H.; Minami, T.; Bonness, S.; Kishi, R.; Takahashi, H.; Kubo, T.; Kamada, K.; Ohta, K.; Champagne, B.; Botek, E. *Chem. Phys. Lett.* **2009**, *477*, 355.
- (11) (a) Srinivas, K.; Prabhakar, Ch.; Lavanya Devi, C.; Yesudas, K.; Bhanuprakash, K.; Jayathirtha Rao, V. *J. Phys. Chem. A* **2007**, *111*, 3378. (b) Anup, T.; Srinivas, K.; Prabhakar, Ch.; Bhanuprakash, K.; Jayathirtha Rao, V. *Chem. Phys. Lett.* **2008**, *454*, 36. (c) Fabian, J. *Chem. Rev.* **1992**, *92*, 1197–1228.
- (12) (a) Yesudas, K.; Bhanuprakash, K. *J. Phys. Chem. A* **2007**, *111*, 1943. (b) Prabhakar, Ch.; Krishna Chaitanya, G.; Sitha, S.; Bhanuprakash, K.; Jayathirtha Rao, V. *J. Phys. Chem. A* **2005**, *109*, 2614. (c) Prabhakar, K.; Yesudas, K.; Bhanuprakash, V.; Jayathirtha Rao, R. S.; Santosh Kumar, D.; Narayana, Rao *J. Phys. Chem. C* **2008**, *112*, 13272.
- (13) (a) Prabhakar, Ch.; Yesudas, K.; Krishna Chaitanya, G.; Sitha, S.; Bhanuprakash, K.; Jayathirtha Rao, V. *J. Phys. Chem. A* **2005**, *109*, 8604. (b) Yesudas, K.; Krishna Chaitanya, G.; Prabhakar, Ch.; Bhanuprakash, K.; Jayathirtha Rao, V. *J. Phys. Chem. A* **2006**, *110*, 11717.
- (14) (a) Cariati, E.; Forni, A.; Biella, S.; Metrangolo, P.; Meyer, F.; Resnati, G.; Righetto, S.; Tordinia, E.; Ugo, R. *Chem. Commun.* **2007**, 2590. (b) Dragonetti, C.; Righetto, S.; Roberto, D.; Ugo, R.; Valore, A.; Fantacci, S.; Sgamellotti, A.; De Angelis, F. *Chem. Commun.* **2007**, 4116. (c) Sanguinet, L.; Williams, J. C.; Yang, Z.; Twieg, R. J.; Mao, G.; Singer, K. D.; Wiggers, G.; Petschek, R. *G. Chem. Mater.* **2006**, *18*, 4259. (d) Cheng, Y.-J.; Luo, J.; Hau, S.; Bale, D. H.; Kim, T.-D.; Shi, Z.; Lao, D. B.; Tucker, N. M.; Tian, Y.; Dalton, L. R.; Reid, P. J.; Jen, A. K.-Y. *Chem. Mater.* **2007**, *19*, 1154.
- (15) (a) Halter, M.; Liao, Y.; Plocinik, R. M.; Coffey, D. C.; Bhattacharjee, S.; Mazur, U.; Simpson, G. J.; Robinson, B. H.; Keller, S. L. *Chem. Mater.* **2008**, *20*, 1778. (b) David, K. S.; Hemeryck, A.; Tancrez, N.; Toupet, L.; Williams, J. A. G.; Ledoux, I.; Zyss, J.; Boucekkine, A.; Guegan, J.-P.; Bozec, H. L.; Maury, O. *J. Am. Chem. Soc.* **2006**, *128*, 12243. (c) Cariati, E.; Macchi, R.; Roberto, D.; Ugo, R.; Galli, S.; Casati, N.; Macchi, P.; Sironi, A.; Bogani, L.; Caneschi, A.; Gatteschi, D. *J. Am. Chem. Soc.* **2007**, *129*, 9410.
- (16) (a) Lamere, J. F.; Lacroix, P. G.; Farfan, N.; Rivera, J. M.; Santillan, R.; Nakatani, K. *J. Mater. Chem.* **2006**, *16*, 2913. (b) Schmidt, K.; Barlow, S.; Leclercq, A.; Zojer, E.; Jang, S.-H.; Marder, S. R.; Jen, A. K.-Y.; Bredas, J.-L. *J. Mater. Chem.* **2007**, *17*, 2944. (c) Zrig, S.; Koeckelberghs, G.; Verbiest, T.; Andrioletti, B.; Rose, E.; Persoons, A.; Asselberghs, I.; Clays, K. *J. Org. Chem.* **2007**, *72*, 5855. (d) Li, Z.; Chen, Z.; Xu, S.; Niu, L.; Zhang, Z.; Zhang, F.; Kasatani, K. *Chem. Phys. Lett.* **2007**, *447*, 110. (e) Yuan, Z.; Entwistle, C. D.; Collings, J. C.; Albesa-Jove, D.; Batsanov, A. S.; Howard, J. A. K.; Taylor, N. J.; Kaiser, H. M.; Kaufmann, D. E.; Poon, S.-Y.; Wong, W.-Y.; Jardin, C.; Fathallah, S.; Boucekkine, A.; Halet, J.-F.; Marder, T. B. *Chem.—Eur. J.* **2006**, *12*, 2758.
- (17) (a) Tatsuura, S.; Tian, M.; Furuki, M.; Sato, Y.; Iwasa, I.; Mitsui, H. *Appl. Phys. Lett.* **2004**, *84*, 1450. (b) Tatsuura, S.; Mastubara, T.; Tian, M.; Mitsui, H.; Iwasa, I.; Sato, Y.; Furuki, M. *Appl. Phys. Lett.* **2004**, *85*, 540.
- (18) (a) Li, Z.; Song, X.; Lei, H.; Xin, H.; Lihong, N.; Zihui, C.; Zhi, Z.; Fushi, Z.; Kazuo, K. *Chem. Phys. Lett.* **2007**, *441*, 123. (b) Li, Z.-Y.; Jin, Z.-H.; Kasatani, K.; Okamoto, H. *Chin. Phys. Lett.* **2005**, *22*, 2282. (c) Dirk, C. W.; Herndon, W. C.; Cervantes-Lee, F.; Selnau, H.; Martinez, S.; Kalamegham, P.; Tan, A.; Campos, G.; Velez, M.; Zyss, J.; Ledoux, I.; Cheng, L.-T. *J. Am. Chem. Soc.* **1995**, *117*, 2214. (d) Tran, K.; Scott, G. W.; Funk, D. J.; Moore, D. S. *J. Phys. Chem.* **1996**, *100*, 11863. (e) Andrews, J. H.; Khaydarov, J. D. V.; Singer, K. D. *Opt. Lett.* **1994**, *19*, 984.
- (19) (a) Srinivas, K.; Sitha, S.; Jayathirtha Rao, V.; Bhanuprakash, K.; Ravikumar, K. *J. Mater. Chem.* **2006**, *16*, 496. (b) Srinivas, K.; Sitha, S.; Jayathirtha Rao, V.; Bhanuprakash, K.; Ravikumar, K.; Philip Anthony, S.; Radhakrishnan, T. P. *J. Mater. Chem.* **2005**, *15*, 965.
- (20) (a) Srinivas, K.; Sitha, S.; Jayathirtha Rao, V.; Bhanuprakash, K. *Opt. Mater.* **2006**, *28*, 1006. (b) Sitha, S.; Srinivas, K.; Raghunath, P.; Bhanuprakash, K.; Jayathirtha Rao, V. *J. Mol. Struct. (Theochem)* **2005**, *728*, 57. (c) Sitha, S.; Laxmikanth Rao, J.; Bhanuprakash, K.; Choudary, B. M. *J. Phys. Chem. A* **2001**, *105*, 8727.
- (21) (a) Enrique, F.-S.; Francisco, J. C.-G.; Angela, S.-S.; Belen, V.; Jesus, O.; Raquel, A.; Fernando, F.-L. *Tetrahedron* **2009**, *65*, 4513. (b) Carlo, T.; Leonardo, D. B.; Sheng, Y.; James, P. R.; Artem, E. M.; Kevin, D. B.; Florencio, E. H. *J. Chem. Phys.* **2009**, *130*, 214504. (c) Wei, Z.-H.; Li, H.-X.; Ren, Z.-G.; Lang, J.-P.; Zhang, Y.; Sun, Z.-R. *Dalton Trans.* **2009**, 3425. (d) Qin, C.; Wang, X.; Wang, J.-J.; Mao, J.; Yang, J.; Dai, L.; Chen, G. *Dyes Pigments* **2009**, *82*, 329. (e) Mario, R.; Jose, L. M.; Gabriel, R.-O.; Jean, F. L.; Pascal, G. L.; Norberto, F.; Ma Eugenia, O.; Rosa, S.; Marco Antonio, M.-N.; Oracio, B.-G.; Keitaro, N. *New J. Chem.* **2009**, *33*, 1693. (f) Hegde, P. K.; Adhikari, A. V.; Manjunatha, M. G.; Suchand Sandeep, C. S.; Philip, R. *Synth. Met.* **2009**, *159*, 1099.
- (22) (a) Law, K. Y. *Chem. Rev.* **1993**, *93*, 449. (b) Law, K. Y. *J. Org. Chem.* **1992**, *57*, 3278. (c) Moustroph, H.; Stollenwerk, M.; Bressau, V. *Angew. Chem., Int. Ed.* **2006**, *45*, 2016. (d) Devi, D. G.; Cibir, T. R.; Ramaiah, D.; Abraham, A. *J. Photochem. Photobiol. B: Biol.* **2008**, *92*, 153.
- (23) (a) Renard, B.-L.; Aubert, Y.; Asseline, U. *Tetrahedron Lett.* **2009**, *50*, 1897. (b) Arunkumar, E.; Forbes, C. C.; Noll, B. C.; Smith, B. D. *J. Am. Chem. Soc.* **2005**, *127*, 3288. (c) Chen, H.; Farahat, M. S.; Law, K.-Y.; Whitten, D. G. *J. Am. Chem. Soc.* **1996**, *118*, 2584. (d) Law, K. Y. *J. Phys. Chem.* **1987**, *91*, 5184. (e) Cano, M. L.; Cozens, F. L.; Esteves, M. A.; Marquez, F.; García, H. *J. Org. Chem.* **1997**, *62*, 7121. (f) Langhals, H. *Angew. Chem., Int. Ed.* **2003**, *42*, 4286.
- (24) (a) Meier, H.; Dullweber, U. *J. Org. Chem.* **1997**, *62*, 4821. (b) Meier, H.; Dullweber, U. *Tetrahedron Lett.* **1996**, *37*, 1191. (c) Meier, H.; Petermann, R.; Gerold, J. *Chem. Commun.* **1999**, 977.
- (25) (a) Simard, T. P.; Yu, J. H.; Zebrowski-Young, J. M.; Haley, N. F.; Detty, M. R. *J. Org. Chem.* **2000**, *65*, 2236. (b) Buschel, M.; Ajayaghosh, A.; Arunkumar, E.; Daub, J. *Org. Lett.* **2003**, *5*, 2975.
- (26) Bigelow, R. W.; Freund, H. *J. Chem. Phys.* **1986**, *107*, 159.
- (27) Gude, C.; Retiig, W. *J. Phys. Chem. A* **2000**, *104*, 8050.
- (28) Ros-Lis, J. V.; Martinez-Manez, R.; Sancenon, F.; Soto, J.; Spieles, M.; Rurack, K. *Chem.—Eur. J.* **2008**, *14*, 10101.
- (29) (a) Fabian, J.; Zahradnik, R. *Angew. Chem. Int. Ed.* **1989**, *28*, 677. (b) Fabian, J. *Dyes Pigments* **2010**, *84*, 36. (c) Dohnert, D.; Koutecky, J. *J. Am. Chem. Soc.* **1980**, *102*, 1790.
- (30) (a) Yang, M.; Jiang, Y. *Phys. Chem. Chem. Phys.* **2001**, *3*, 167. (b) Ohira, S.; Rudra, I.; Schmidt, K.; Barlow, S.; Chung, S.-J.; Zhang, Q.; Matichak, J.; Marder, S. R.; Bredas, J.-L. *Chem.—Eur. J.* **2008**, *14*, 11082. (c) Yang, M.; Jiang, Y. *Phys. Chem. Chem. Phys.* **2001**, *3*, 4213. (d) Yang, M.; Jiang, Y. *Chem. Phys.* **2001**, *274*, 121.
- (31) Nalwa, H. S.; Hanack, M.; Pawlowski, G.; Engel, M. K. *Chem. Phys.* **1999**, *245*, 17.
- (32) (a) Terenziani, F.; Katan, C.; Badaeva, E.; Tretiak, S.; Blanchard-Desce, M. *Adv. Mater.* **2008**, *20*, 4641. (b) Ibersiene, F.; Hammoutène, D.; Boucekkine, A.; Katan, C.; Blanchard-Desce, M. *J. Mol. Struct. (Theochem)* **2008**, *866*, 58. (c) Terenziani, F.; Mongin, O.; Katan, C.; Bhatthula, B. K. G.; Blanchard-Desce, M. *Chem.—Eur. J.* **2006**, *12*, 3089.
- (33) (a) Park, S. Y.; Jun, K.; Oh, S.-W. *Bull. Korean Chem. Soc.* **2005**, *26*, 428. (b) Rong, J.; Peng, Y.; Roesky, H. W.; Li, J.; Vidovic, D.; Magull, J. *Eur. J. Inorg. Chem.* **2003**, 3110. (c) Ehrhardt, H.; Hunig, S.; Putter, H. *Chem. Ber.* **1977**, *110*, 2506. (d) Forster, M.; Hester, R. E. *J. Chem. Soc., Faraday Trans.* **1982**, *78*, 1847.
- (34) Frisch, M. J.; Trucks, G. W.; Schlegel, H. B.; Scuseria, G. E.; Robb, M. A.; Cheeseman, J. R.; Montgomery, Jr. J. A.; Vreven, T.; Kudin, K. N.; Burant, J. C.; Millam, J. M.; Iyengar, S. S.; Tomasi, J.; Barone, V.; Mennucci, B.; Cossi, M.; Scalmani, G.; Rega, N.; Petersson, G. A.; Nakatsuji, H.; Hada, M.; Ehara, M.; Toyota, K.; Fukuda, R.; Hasegawa, J.; Ishida, M.; Nakajima, T.; Honda, Y.; Kitao, O.; Nakai, H.; Klene, M.; Li, X.; Knox, J. E.; Hratchian, H. P.; Cross, J. B.; Adamo, C.; Jaramillo, J.; Gomperts, R.; Stratmann, R. E.; Yazyev, O.; Austin, A. J.; Cammi, R.; Pomelli, C.; Ochterski, J. W.; Ayala, P. Y.; Morokuma, K.; Voth, G. A.; Salvador, P.; Dannenberg, J. J.; Zakrzewski, V. G.; Dapprich, S.; Daniels, A. D.; Strain, M. C.; Farkas, O.; Malick, D. K.; Rabuck, A. D.; Raghavachari, K.; Foresman, J. B.; Ortiz, J. V.; Cui, Q.; Baboul, A. G.; Clifford, S.; Cioslowski, J.; Stefanov, B. B.; Liu, G.; Liashenko, A.; Piskorz, P.; Komaromi, I.; Martin, R. L.; Fox, D. J.; Keith, T.; Al-Laham, M. A.; Peng, C. Y.; Nanayakkara, A.; Challacombe, M.; Gill, P. M. W.; Johnson, B.; Chen, W.; Wong, M. W.; Gonzalez, C.; Pople, J. A.; *Gaussian 03*, revision 01; Gaussian, Inc.: Wallingford, CT, 2004.
- (35) (a) Nakajima, T.; Nakatsuji, H. *Chem. Phys. Lett.* **1997**, *280*, 79. (b) Ishida, M.; Toyota, K.; Ehara, M.; Nakatsuji, H. *Chem. Phys. Lett.* **2001**, *347*, 493. (c) Nakajima, T.; Nakatsuji, H. *Chem. Phys. Lett.* **1999**, *242*, 177. (d) Nakajima, T.; Nakatsuji, H. *Chem. Phys. Lett.* **1999**, *300*, 1. (e) Wan, J.; Ehara, M.; Hada, M.; Nakatsuji, H. *J. Chem. Phys.* **2000**, *113*, 5245. (f) Wan, J.; Hada, M.; Ehara, M.; Nakatsuji, M. *J. Chem. Phys.* **2001**, *114* (2), 842. (g) Nakatsuji, H. *Acta Chim. Hungar., Models Chem.* **1992**, *129*, 719. (h) Nakatsuji, H. In *Computational Chemistry-Reviews of Current Trends*; Leszczynski, J., Ed.; World Scientific: Singapore, 1997; Vol. 2.
- (36) Hu, Z.; Boyd, R. J.; Nakatsuji, H. *J. Am. Chem. Soc.* **2002**, *124*, 2664.
- (37) Wyrz, J. *Pure Appl. Chem.* **1984**, *56*, 1289.
- (38) Nakano, M.; Nitta, T.; Yamaguchi, K.; Champagne, B.; Botek, E. *J. Phys. Chem. A* **2004**, *108*, 4105.
- (39) (a) Yamaguchi, K. *Self-Consistent Field Theory and Applications*; Carbo, R.; Klobukowski, M., Eds.; Elsevier: Amsterdam, 1990; p 727. (b) Yamanaka, S.; Okumura, M.; Nakano, M.; Yamaguchi, K. *J. Mol. Struct. (Theochem)* **1994**, *310*, 205.
- (40) (a) Kamada, K.; Ueda, M.; Nagao, H.; Tawa, K.; Takushi, S.; Shmizu, Y.; Ohta, K. *J. Phys. Chem. A* **2000**, *104*, 4723, and references cited therein. (b) Kurtz, H. A.; Stewart, J. P.; Dieter, K. M. *J. Comput. Chem.* **1990**, *11*, 82.
- (41) Breher, F. *Coord. Chem. Rev.* **2007**, *251*, 1007.

(42) (a) Stoll, R. S.; Severin, N.; Rabe, J. P.; Hecht, S. *Adv. Mater.* **2006**, *18*, 1271. (b) Alex, S.; Basheer, M. C.; Arun, K. T.; Ramaiah, D.; Das, S. *J. Phys. Chem. A* **2007**, *111*, 3226.

(43) (a) Griffiths, J.; Mama, J. *Dyes Pigments* **2000**, *44*, 9. (b) Lopes, J. G. S.; Farani, R. A.; de Oliveira, L. F. C.; Santos, P. S. *J. Raman Spectrosc.* **2006**, *37*, 142.

(44) (a) Marek, S.; Anna, S.; Barry, L.-D.; Zhenan, B.; Luping, Y.; Bing, H.; Ullrich, S. *J. Opt. Soc. Am. B* **1998**, *15*, 817. (b) Mingtang, Z.; Yiping,

C.; Marek, S.; Prasad, P. N.; Marilyn, R. U.; Bruce, A. R. *J. Chem. Phys.* **1991**, *95*, 3991.

(45) (a) Sheik-Bahae, M.; Said, A. A.; Wei, T.; Hagan, D. J.; Van Stryland, E. W. *IEEE J. Quant. Electron.* **1990**, *26*, 760. (b) Gu, B.; Huang, X.-Q.; Tan, S.-Q.; Wang, M.; Ji, W. *Appl. Phys. B: Laser Opt.* **2009**, *9*, 375.

JP908475N